ChemComm

Check for updates

Octacyano-substituted tridecacyclene: a non-benzenoid cyanocarbon with low-lying LUMO and multistage redox properties†

Erik Misselwitz, Jonas Spengler, [ID] Frank Rominger and Milan Kivala [ID] *

Octacyanated tridecacyclene was synthesized from novel brominated tridecacyclene. In the crystal, the saddle-shaped scaffold exhibits a zigzag packing motif governed by an interplay between the inherent geometry of the central cyclooctatetraene moiety and the hydrogen bonding mediated by the dipolar cyano functionalities. The compound undergoes five reversible reductions in a particularly narrow potential window of 1.15 V in CH_2Cl_2. The first reduction occurs at -0.78 V (*vs.* Fc/Fc$^+$), which corresponds to a remarkably low-lying LUMO of -4.32 eV.

The discovery of conductive charge-transfer complexes between 7,7,8,8-tetracyanoquinodimethane (TCNQ) and tetrathiafulvalene (TTF) back in the 1970s[1] sparked intense research towards novel electron acceptors. The decoration of various π-conjugated frameworks with strongly electron-withdrawing cyano groups was identified as a particularly potent strategy affording the family of so-called cyanocarbons.[2] In these compounds, the highly dipolar cyano group with its cylindrical shape undergoes efficient conjugation with the adjacent π system and modulates its optoelectronic properties while rendering it electron deficient (Hammett constant σ_p(CN) = +0.66).[3] The resulting cyanocarbons are highly reactive electrophiles often showing unusual modes of reactivity. Moreover, the partially negative nitrogen with its lone pair can coordinate to metal centers,[4] and participate in hydrogen[5] or halogen[6] bonding, while the cyano moiety is prone to dipolar CN···CN interactions.[7] Programmed combination of these directional noncovalent interactions enabled the self-assembly of highly-organized architectures of various dimensions.[8] These appealing attributes of cyanocarbons and cyano-functionalized π-systems allowed the development of electron-deficient molecular materials with unique optoelectronic properties and supramolecular behaviour.[9,10]

Organisch-Chemisches Institut, Universität Heidelberg, Im Neuenheimer Feld 270, 69120 Heidelberg, Germany. E-mail: milan.kivala@oci.uni-heidelberg.de

† Electronic supplementary information (ESI) available: Experimental, analytical, computational and crystallographic details. CCDC 2421984 (**T-Br**) and 2421985 (**T-CN**). For ESI and crystallographic data in CIF or other electronic format see DOI: https://doi.org/10.1039/d5cc00672d

The incorporation of non-benzenoid rings into the sp^2-carbon frameworks of polycyclic aromatic hydrocarbons (PAHs) represents a complementary approach to achieve new types of carbonaceous electron acceptors.[11] In particular, the conjugated 5-membered rings are highly beneficial due to the aromatic stabilization of the corresponding cyclopentadienyl-like anion, facilitating the electron uptake.[12] Similarly, 8-membered cyclooctatetraene (COT) with its saddle-shaped geometry, imparts redox activity by aromatic stabilization of the respective planarized 6 π-electron dication and 10 π-electron dianion.[13] Tridecacyclene[14,15] (**T**) combining both the 5- and 8-membered carbocycles in its structure has been used for the development of strong electron acceptors prone to multiple reduction events such as tridecacyclene tetraimide[16] (**T-Im**) and indenoannulated tridecacyclene[17] (**T-Ind**), which was recently developed in our group (Fig. 1).

However, non-benzenoid PAHs with multiple cyano groups are comparably scarce and the known representatives are almost exclusively based on corannulene.[18]
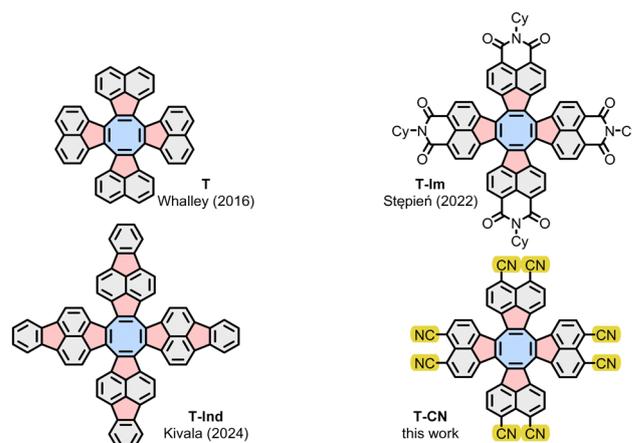

Fig. 1 Representative electron acceptors derived from tridecacyclene (**T**),[14] including tridecacyclene tetraimide (**T-Im**)[16] and indenoannulated tridecacyclene (**T-Ind**)[17] and the title compound **T-CN** reported herein.

In this work, we have developed an unprecedented non-benzenoid cyanocarbon (**T-CN**) through decoration of the inherently redox-active tridecacyclene scaffold with multiple strongly electron-withdrawing cyano groups. The compound undergoes five reversible reductions under electrochemical conditions and exhibits a unique packing motif in the solid state, which is dictated by an interplay between the dipolar cyano moieties and the saddle-shaped geometry of the tridecacyclene scaffold.

The key precursor in the synthesis of **T-CN** was dibrominated acenaphthenone **1**, which was obtained in an overall yield of 15% over two steps from commercially available acenaphthene (for synthetic details, see ESI†). Compound **1** was subjected to a Lewis acid-mediated cyclomerization with $TiCl_4$ at elevated temperature to afford octabrominated tridecacyclene **T-Br** in 31% yield as a dark brown solid (Scheme 1). Notably, under these conditions the formation of the corresponding cyclotrimer or higher oligomers was not observed. The constitution of **T-Br** was confirmed by X-ray crystallography (see ESI†). In contrast to tetrabrominated tridecacyclene, which was reported previously by our group and which only occurs as an inseparable mixture of regioisomers,[17] **T-Br** features a considerably higher synthetic potential as a versatile precursor for non-benzenoid PAHs. The initially attempted cyanation under Rosenmund-von Braun conditions[8] failed and only the Pd-catalysed protocol[9d] using CuCN as the cyanide source, delivered octacyano-substituted **T-CN** as a brown solid in 7% yield (*i.e.*, *ca.* 72% per cyanation step) after chromatography.

Single crystals of **T-CN** suitable for X-ray diffraction were obtained by slow evaporation of a saturated solution of **T-CN** in nitrobenzene-d_5 at room temperature. The bond lengths of the tridecacyclene core are only slightly affected by the cyano substitution and are similar to those of pristine tridecacyclene (**T**).[14] However, the cyano groups exert a strong impact on both the overall geometry and the packing behaviour of **T-CN** that strongly differ from the parent **T**. **T-CN** features an almost ideal D_{2d} symmetric structure with angles between the two mean planes defined by all carbon atoms of the opposing acenaphthylene subunits of 102.5° and 103.0° compared to 102.9° and 105.4° reported for **T**[14] (Fig. 2A). While in the solid-state packing of **T**, the neighbouring molecules interact *via* π···π interactions between the acenaphthylene subunits, **T-CN** shows a markedly different behaviour and forms a complex motif upon multiple
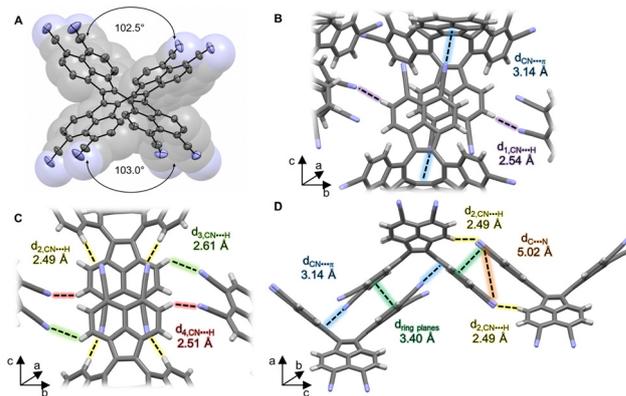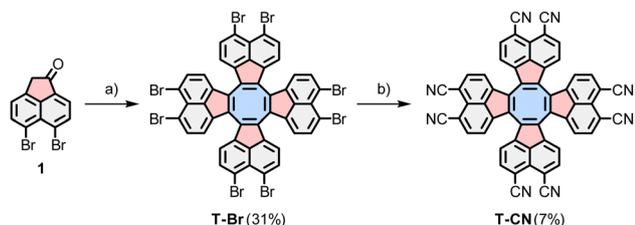

Fig. 2 X-ray crystallographic structure of **T-CN**. (A) Side view of an individual molecule. (B) and (C) Top view of the intermolecular interactions between two neighbouring molecules. (D) The zigzag packing motif apparent along the *c* axis. The angles and distances calculated upon the mean planes defined by the acenaphthylene moieties; ellipsoids at 50% probability level, hydrogen atoms and solvent molecules omitted for clarity.

short contacts involving the cyano groups of eight neighbouring **T-CN** molecules (see ESI†). The most distinct interactions occur along the crystallographic *c* axis, where one molecule of **T-CN** interacts through two orthogonally oriented acenaphthylene flanks at a distance of 3.40 Å (3.44 Å for **T**).[14] The cyano groups are engaged in hydrogen bonding interactions[5,9c,19] ($d_{CN···H}$ = 2.49–2.61 Å) as well as CN···π interactions[20] ($d_{CN···π}$ = 3.14 Å) with the upwards pointing acenaphthylene moieties of the neighbouring molecules (Fig. 2B and C).[7] Characteristic short contacts indicating the occurrence of dipolar interactions between the cyano groups are not observed.[7] Overall, the supramolecular organisation of **T-CN**, which is additionally stabilized by CN···H–C(sp^2) hydrogen bonding along the crystallographic *a* axis (see ESI†), results in an apparent zigzag pattern along the crystallographic *c* axis (Fig. 2D).

To probe the influence of the cyanation on the optoelectronic properties of the tridecacyclene core, UV-Vis absorption spectra of **T-CN** and **T** were recorded in CH_2Cl_2 at rt (Fig. 3A). While the overall spectral features remain similar, the cyanation redshifts the longest wavelength absorption maximum (λ_{max}) by 27 nm from 430 nm (for **T**) to 457 nm (for **T-CN**). The molar extinction coefficient of **T-CN** is similar to that of **T**

Scheme 1 Synthesis of octacyanated tridecacyclene **T-CN**. Reagents and conditions: (a) $TiCl_4$, *o*-DCB, 200 °C, 30 min; (b) $[Pd_2(dba)_3]$, dppf, CuCN, 1,4-dioxane, 50 °C, 48 h. *o*-DCB = 1,2-dichlorobenzene, dba = dibenzylideneacetone, dppf = 1,1′-bis(diphenylphosphino)ferrocene.
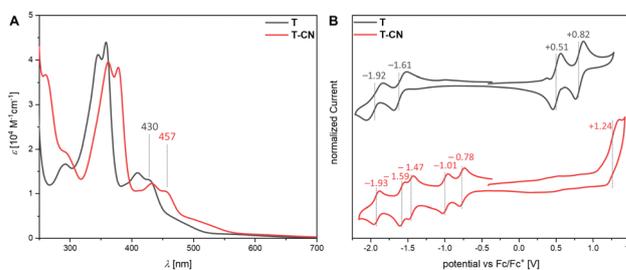

Fig. 3 (A) UV-Vis absorption spectra of **T** and **T-CN** (CH_2Cl_2). (B) Cyclic voltammograms of **T** and **T-CN** (CH_2Cl_2, nBu$_4$NPF$_6$ (0.1 M), c = 2 mM, ν = 149 mV s^{-1}).

Table 1 Experimental photophysical and electrochemical data and calculated HOMO and LUMO energies for **T-CN** and **T**

	$\lambda_{max}/\lambda_{on}{}^{ab}$ [nm]	$E_g^{opt\,c}$ [eV]	$E_{HOMO,DFT}/E_{LUMO,DFT}{}^d$ [eV]	$E_{ox,CV}/E_{red,CV}{}^e$ [V]	$E_{HOMO,CV}/E_{LUMO,CV}{}^f$ [eV]
T	430/529	2.34	−5.14/−2.78	+0.82, +0.51/−1.61, −1.92	−5.61/−3.49
T-CN	457/579	2.14	−6.87/−4.70	+1.24/−0.78, −1.01, −1.47, −1.59, −1.93	−6.34/−4.32

^{a} Recorded in CH_2Cl_2 at rt. ^{b} λ_{on} estimated using the tangent method. ^{c} Optical band gap $E_g^{opt} = hc/\lambda_{on}$. ^{d} DFT calculated values (B3LYP(D3BJ)/6311G+(d,p)). ^{e} Measured in CH_2Cl_2 vs. Fc/Fc$^+$ at rt. ^{f} Calculated from $E_{HOMO,CV} = -5.1$ eV $- E_{ox,1}$ and $E_{LUMO,CV} = -(E_{red,1} + 5.1$ eV); oxidation potential of Fc against vacuum is set at 5.1 eV.[24]

(see Table 1). Time-dependent density functional theory (TD-DFT) calculations (CAM-B3LYP[21](D3BJ)[22]/6-311G+(d,p)[23]) reproduce well the experimentally observed spectra (see ESI†). The lowest energy absorption maxima of both compounds are characterized by a major contribution from a HOMO→LUMO+1 transition and a HOMO→LUMO+2 transition exhibiting the same excitation energy.

The redox properties were investigated by cyclic voltammetry (CV), differential pulse voltammetry (DPV) and square-wave voltammetry (SWV) in CH_2Cl_2 at rt (Fig. 3B and ESI†). **T-CN** displays six redox events including five reversible reductions between −0.78 V and −1.93 V and one irreversible oxidation at +1.24 V (vs. ferrocene/ferrocenium (Fc/Fc$^+$)). In contrast, parent **T** only shows four reversible redox events under analogous conditions within the available potential window of CH_2Cl_2, including two reductions (−1.61 V and −1.92 V) and two oxidations (+0.51 V and +0.82 V). Hence, the cyanation of **T** results in a dramatic anodic shift of the first reduction of **T-CN** by 830 mV and the occurrence of the three additional reduction steps. Notably, the five reductions of **T-CN** occur within a remarkably narrow potential range of only 1.15 V (1.10 V for the first five reductions of **T-Im**), with the first reduction at −0.78 V being even more positive than for **T-Im** (−0.88 V vs. Fc/Fc$^+$ in THF).[16] The HOMO and LUMO energy levels of −6.34 eV and −4.32 eV, respectively, were estimated from the electrochemical data for **T-CN** and compared to parent **T** in Table 1.[24]

DFT calculations (B3LYP[25](D3BJ)[22]/6-311G+(d,p)[23]) yielded −6.87 eV and −4.70 eV for the HOMO and LUMO, respectively (Fig. 4A), which is in good agreement with the values extracted from the electrochemical data. Hence, the 8-fold cyanation leads to a dramatic lowering of both the LUMO and the HOMO by 1.92 eV and 1.73 eV, respectively, compared to parent **T**. This evolution translates into a narrowing of the calculated HOMO–LUMO energy gap by 0.19 eV when going from **T** to **T-CN**. However, the shape and localization of the orbitals remains largely unaffected, which also indicates the comparable extent of π-electron delocalization and aromaticity in both **T** and **T-CN**, as probed by nucleus independent chemical shift (NICS) calculations (Fig. 4B). The harmonic oscillator model of aromaticity (HOMA)[26] values based on the experimental bond lengths from X-ray crystallography further corroborate the NICS trends, indicating the weak antiaromatic character of the 5- and 8-membered rings. Motivated by the rich reversible redox behavior of **T-CN** observed under electrochemical conditions, its chemical reduction with sodium metal ($E_0 = -3.04$ V vs. Fc/Fc$^+$)[27] in the presence of 18-crown-6 in THF was conducted
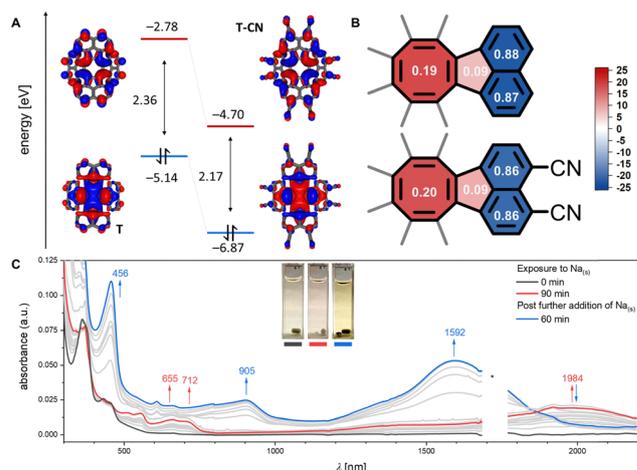

Fig. 4 (A) Kohn−Sham molecular orbitals (0.02 e$^{1/2}$ Bohr$^{-3/2}$ isosurfaces) of **T-CN** and **T** (B3LYP(D3BJ)/6311G+(d,p)). (B) Schematic depiction of the NICS(1)$_{zz-av}$ values of **T-CN** and **T** (for the numerical values of NICS(1)$_{zz-av}$, see ESI†) and HOMA values of **T-CN** and **T** based on the crystal structure. (C) Reduction of **T-CN** with an excess of sodium metal in the presence of 18-crown-6 in THF monitored by UV-Vis-NIR absorption spectroscopy. Red and blue traces correspond to maximum concentrations of **T-CN$^{•-}$** and **T-CN^{2-}**, respectively. *Data points between 1684 and 1773 nm are omitted due to solvent absorption.

to investigate the optoelectronic properties of the anionic species by UV-Vis-NIR spectroscopy (Fig. 4C). Addition of sodium metal initially results in a color change of the solution from light brown to pale purple and the emergence of several new absorption bands, with prominent absorptions centered around 655, 712 and 1984 nm. The occurrence of an isosbestic point indicates the clean conversion of **T-CN** to the corresponding anion. Further addition of sodium metal resulted in several new absorption maxima centered at 456, 905 and 1592 nm, corresponding to a color change to pale green. Further extension of the reaction time to 5 h resulted in a decreased intensity of the spectral features, which completely vanished after 20 h, indicating the decomposition of the reduced species (see ESI†). Nearly identical spectral features were observed in spectroelectrochemical studies (see ESI†). The absorptions were qualitatively reproduced by TD-DFT calculations which, supported by literature data on related tridecacyclene-based systems,[15–17] allowed the observed spectral features to be assigned to the radical anion **T-CN$^{•-}$** and the dianion **T-CN^{2-}** (see ESI†).

In summary, we have developed a new non-benzenoid cyanocarbon, which was accessible through a Pd-catalyzed 8-fold

cyanation of brominated tridecacyclene. The compound crystallizes in an apparent zigzag packing motif governed by the interplay between the spatial requirements of the octagon-centered polycyclic scaffold and the hydrogen bonding involving the dipolar cyano moieties. The strongly electron-withdrawing cyano groups render the scaffold a multistage electron acceptor with a low-lying LUMO, which is capable of five reversible reductions within an exceptionally narrow potential range of 1.15 V under electrochemical conditions. The anionic species generated by the reduction with sodium metal exhibit broad bathochromically shifted absorptions in the UV-Vis-NIR spectra. Our results highlight the potential of combining non-benzenoid rings with cyano groups to generate a new type of cyanocarbons with a high electron affinity and a unique solid-state structure.

Data availability

The data supporting this article have been included as part of the ESI.†

Conflicts of interest

There are no conflicts to declare.

Notes and references

1 J. Ferraris, D. O. Cowan, V. Walatka and J. H. Perlstein, *J. Am. Chem. Soc.*, 1973, **95**, 948–949.
2 O. W. Webster, *J. Polym. Sci. A Polym. Chem.*, 2002, **40**, 210–221.
3 C. Hansch, A. Leo and R. W. Taft, *Chem. Rev.*, 1991, **91**, 165–195.
4 S. Benmansour, C. Atmani, F. Setifi, S. Triki, M. Marchivie and C. J. Gómez-García, *Coord. Chem. Rev.*, 2010, **254**, 1468–1478.
5 S. Mahapatra, Y. Azim and G. R. Desiraju, *J. Mol. Struct.*, 2010, **976**, 200–204.
6 A. Sun, J. W. Lauher and N. S. Goroff, *Science*, 2006, **312**, 1030–1034.
7 P. A. Wood, S. J. Borwick, D. J. Watkin, W. D. S. Motherwell and F. H. Allen, *Acta Crystallogr. B*, 2008, **64**, 393–396.
8 K. Müller, J. C. Moreno-López, S. Gottardi, U. Meinhardt, H. Yildirim, A. Kara, M. Kivala and M. Stöhr, *Chem. – Eur. J.*, 2016, **22**, 581–589.
9 (a) H. Wang, C. Zhao, Z. Burešová, F. Bureš and J. Liu, *J. Mater. Chem. A*, 2023, **11**, 3753–3770; (b) L. Ueberricke, I. Ciubotaru, F. Ghalami, F. Mildner, F. Rominger, M. Elstner and M. Mastalerz, *Chem. – Eur. J.*, 2020, **26**, 11634–11642; (c) J. Chang, Q. Ye, K.-W. Huang, J. Zhang, Z.-K. Chen, J. Wu and C. Chi, *Org. Lett.*, 2012, **14**, 2964–2967; (d) Q. Ye, J. Chang, K.-W. Huang, X. Shi, J. Wu and C. Chi, *Org. Lett.*, 2013, **15**, 1194–1197.
10 (a) W. R. Hertler, W. Mahler, L. R. Melby, J. S. Miller, R. E. Putscher and O. W. Webster, *Mol. Cryst. Liq. Cryst.*, 1989, **171**, 205–216; (b) J. S. Miller, A. J. Epstein and W. M. Reiff, *Chem. Rev.*, 1988, **88**, 201–220; (c) K. P. Goetz, D. Vermeulen, M. E. Payne, C. Kloc,

L. E. McNeil and O. D. Jurchescu, *J. Mater. Chem. C*, 2014, **2**, 3065–3076.
11 (a) Y. Fei and J. Liu, *Adv. Sci.*, 2022, **9**, e2201000; (b) G. González Miera, S. Matsubara, H. Kono, K. Murakami and K. Itami, *Chem. Sci.*, 2022, **13**, 1848–1868; (c) M. C. Stuparu, *Acc. Chem. Res.*, 2021, **54**, 2858–2870; (d) M. A. Majewski and M. Stępień, *Angew. Chem., Int. Ed.*, 2019, **58**, 86–116; (e) I. R. Márquez, S. Castro-Fernández, A. Millán and A. G. Campaña, *Chem. Commun.*, 2018, **54**, 6705–6718; (f) M. Rickhaus, M. Mayor and M. Juríček, *Chem. Soc. Rev.*, 2017, **46**, 1643–1660; (g) P. Pakulski, M. Magott, S. Chorazy, M. Sarewicz, M. Srebro-Hooper, D. Tabor, Ł. Łapok, D. Szczepanik, S. Demir and D. Pinkowicz, *Chem*, 2024, **10**, 971–997.
12 (a) K. Plunkett, *Synlett*, 2013, 898–902; (b) J. D. Wood, J. L. Jellison, A. D. Finke, L. Wang and K. N. Plunkett, *J. Am. Chem. Soc.*, 2012, **134**, 15783–15789; (c) F. G. Brunetti, X. Gong, M. Tong, A. J. Heeger and F. Wudl, *Angew. Chem., Int. Ed.*, 2010, **49**, 532–536; (d) H. Xia, D. Liu, X. Xu and Q. Miao, *Chem. Commun.*, 2013, **49**, 4301–4303.
13 (a) H. S. Kaufmann, I. Fankuchen and H. Mark, *Nature*, 1948, **161**, 165; (b) T. J. Katz, *J. Am. Chem. Soc.*, 1960, **82**, 3784–3785; (c) G. A. Olah, J. S. Staral, G. Liang, L. A. Paquette, W. P. Melega and M. J. Carmody, *J. Am. Chem. Soc.*, 1977, **99**, 3349–3355.
14 D. P. Sumy, N. J. Dodge, C. M. Harrison, A. D. Finke and A. C. Whalley, *Chem. – Eur. J.*, 2016, **22**, 4709–4712.
15 D. P. Sumy, A. D. Finke and A. C. Whalley, *Chem. Commun.*, 2016, **52**, 12368–12371.
16 R. Kumar, P. J. Chmielewski, T. Lis, D. Volkmer and M. Stępień, *Angew. Chem., Int. Ed.*, 2022, **61**, e202207486.
17 E. Misselwitz, J. Spengler, F. Rominger and M. Kivala, *Chem. – Eur. J.*, 2024, e202400696.
18 (a) D. Hellwinkel, H.-J. Hasselbach and F. Lämmerzahl, *Angew. Chem., Int. Ed. Engl.*, 1984, **23**, 705–706; (b) A. Haupt, R. Walter, B. Loll and D. Lentz, *Eur. J. Org. Chem.*, 2018, 6338–6342; (c) R. Zhu, Z. Liu, J. Chen, X. Xiong, Y. Wang, L. Huang, J. Bai, Y. Dang and J. Huang, *Org. Lett.*, 2018, **20**, 3161–3165; (d) R. Chen, R.-Q. Lu, K. Shi, F. Wu, H.-X. Fang, Z.-X. Niu, X.-Y. Yan, M. Luo, X.-C. Wang, C.-Y. Yang, X.-Y. Wang, B. Xu, H. Xia, J. Pei and X.-Y. Cao, *Chem. Commun.*, 2015, **51**, 13768–13771; (e) Y.-L. Wu, M. C. Stuparu, C. Boudon, J.-P. Gisselbrecht, W. B. Schweizer, K. K. Baldridge, J. S. Siegel and F. Diederich, *J. Org. Chem.*, 2012, **77**, 11014–11026.
19 J. Janczak and R. Kubiak, *Acta Crystallogr., Sect. C*, 1995, **51**, 1399–1401.
20 M. D. Stephenson and M. J. Hardie, *Cryst. Growth Des.*, 2006, **6**, 423–432.
21 T. Yanai, D. P. Tew and N. C. Handy, *Chem. Phys. Lett.*, 2004, **393**, 51–57.
22 (a) S. Grimme, J. Antony, S. Ehrlich and H. Krieg, *J. Chem. Phys.*, 2010, **132**, 154104; (b) S. Grimme, S. Ehrlich and L. Goerigk, *J. Comput. Chem.*, 2011, **32**, 1456–1465.
23 (a) T. Clark, J. Chandrasekhar, G. W. Spitznagel and P. V. R. Schleyer, *J. Comput. Chem.*, 1983, **4**, 294–301; (b) R. Krishnan, J. S. Binkley, R. Seeger and J. A. Pople, *J. Chem. Phys.*, 1980, **72**, 650–654.
24 (a) C. M. Cardona, W. Li, A. E. Kaifer, D. Stockdale and G. C. Bazan, *Adv. Mater.*, 2011, **23**, 2367–2371; (b) A. J. Bard and L. R. Faulkner, *Electrochemical methods. Fundamentals and applications*, Wiley, New York, Weinheim, 2nd edn, 2001; (c) W. N. Hansen and G. J. Hansen, *Phys. Rev. A*, 1987, **36**, 1396–1402; (d) S. Trasatti, *Pure Appl. Chem.*, 1986, **58**, 955–966.
25 (a) P. J. Stephens, F. J. Devlin, C. F. Chabalowski and M. J. Frisch, *J. Phys. Chem.*, 1994, **98**, 11623–11627; (b) A. D. Becke, *J. Chem. Phys.*, 1993, **98**, 5648–5652; (c) C. Lee, W. Yang and R. G. Parr, *Phys. Rev. B: Condens. Matter*, 1988, **37**, 785–789; (d) S. H. Vosko, L. Wilk and M. Nusair, *Can. J. Phys.*, 1980, **58**, 1200–1211.
26 (a) J. Kruszewski and T. M. Krygowski, *Tetrahedron Lett.*, 1972, **13**, 3839–3842; (b) T. M. Krygowski and M. K. Cyrański, *Chem. Rev.*, 2001, **101**, 1385–1419.
27 N. G. Connelly and W. E. Geiger, *Chem. Rev.*, 1996, **96**, 877–910.